1 Modeling Crack Singularities in FEM/X-FEM

In this section, we first present a brief overview of the different approaches used to model stress singularities in finite elements, with particular attention to cracks in isotropic and bimaterial media. Then, we indicate the enrichment functions to be used in the X-FEM to model an interface crack. These enrichment functions span the asymptotic crack-tip fields (see the Appendix) for a crack at the interface between two isotropic linear elastic materials.

1.1 Crack-tip elements in FEM

1.1.1 Isotropic media

In linear elastic fracture mechanics (LEFM), the stresses and strains are inverse square-root singular at the crack-tip. In other words, the stresses and strains vary as $r^{-1/2}$ in the vicinity of the crack-tip, where r is the radial distance from the crack-tip, i.e. $\sigma_{ij} \sim r^{-\lambda}$, where $\lambda = 1/2$ is the exponent. In order to accurately compute fracture parameters such as the stress intensity factor, the eight-node quarter-point element as well as the six-node (collapsed quadrilateral) quarter-point element were introduced (Henshell and Shaw 1975; Barsoum 1976; Barsoum 1977). The quarter-point element introduces the $r^{-1/2}$ behavior in the strains and stresses in the crack-tip element. Efforts have also been made to embed arbitrary-order singularities ($r^{-\lambda}$, $0 < \lambda < 1$) in the vicinity of the crack-tip (Akin 1976; Benzley 1974; Tracey and Cook 1977; Gifford and Hilton 1978; Stern 1979; Hughes and Stern 1980). We now introduce some preliminaries regarding differential geometric considerations and then present the conditions under which singularities in the displacement-derivatives may arise within the finite element method.

Typically, in Galerkin finite elements, the concept of isoparametric mapping is used—both the geometry and the dependent variable $\mathbf{u}$ are mapped via the same interpolation (shape) functions from the reference (parent) space $\boldsymbol{\xi}$ to the physical space $\mathbf{x}$. Consider the mapping $\mathbf{x} : \Box \to \Omega$ shown in Figure 1 for an isoparametric eight-node quadrilateral element:

$$\mathbf{x} = \mathbf{x}(\boldsymbol{\xi}) = \sum_{i=1}^{8} N_i(\boldsymbol{\xi})\mathbf{x_i}\,, \tag{1}$$

where $\mathbf{x} \equiv (x,\, y)$, $\boldsymbol{\xi} \equiv (\xi,\, \eta)$, and the shape functions $N_i(\xi,\, \eta)$ for the eight-node serendipity element are given in Barsoum (1976).

By virtue of the isoparametric assumption, we can represent the displacement (dependent variable) $\mathbf{u}$, where $\mathbf{u} \equiv (u,\, v)$, by a similar equation to that given in Eq. (1):

$$\mathbf{u}(\boldsymbol{\xi}) = \sum_{i=1}^{8} N_i(\boldsymbol{\xi})\mathbf{u_i}\,. \tag{2}$$

Now, by the chain rule of differentiation, we can relate the derivatives of u (similar expressions for v too) in the parent element to that in the physical element by

$$\frac{\partial u}{\partial \xi} = \frac{\partial u}{\partial x}\frac{\partial x}{\partial \xi} + \frac{\partial u}{\partial y}\frac{\partial y}{\partial \xi}\,, \tag{3}$$

which can be written in compact form as

$$\left\{ \begin{array}{c} \dfrac{\partial u}{\partial \xi} \\ \\ \dfrac{\partial u}{\partial \eta} \end{array} \right\} = [\mathbf{J}] \left\{ \begin{array}{c} \dfrac{\partial u}{\partial x} \\ \\ \dfrac{\partial u}{\partial y} \end{array} \right\}, \tag{4}$$

where $[\mathbf{J}]$ is the Jacobian of the transformation given in Eq. (1). Since we need the Cartesian derivatives of u, on inverting the above equation, we obtain

$$\left\{ \begin{array}{c} \dfrac{\partial u}{\partial x} \\ \\ \dfrac{\partial u}{\partial y} \end{array} \right\} = [\mathbf{J}]^{-\mathbf{1}} \left\{ \begin{array}{c} \dfrac{\partial u}{\partial \xi} \\ \\ \dfrac{\partial u}{\partial \eta} \end{array} \right\}. \tag{5}$$

From Eq. (5), it is evident that the singularity in the displacement derivatives at the crack-tip may be introduced in one of three ways:

1. $[\mathbf{J}]$ is singular at the crack-tip. This implies a singularity in the Jacobian of the geometric transformation $\mathbf{x} = \mathbf{x}(\boldsymbol{\xi})$ given in Eq. (1), i.e., $\texttt{det}\ \mathbf{J} = 0$ at the crack-tip. This approach is used in the quarter-point element (Henshell and Shaw 1975; Barsoum 1976), in which the mid-side node in a eight-node quadrilateral (or six-noded triangular) element is moved to the quarter-position (Figure 2).

2. The partial derivatives $\frac{\partial u}{\partial \xi}$ and $\frac{\partial u}{\partial \eta}$ are singular. This corresponds to the introduction of shape functions $N_i(\xi,\, \eta)$ that have singular derivatives with respect to $(\xi,\, \eta)$ (Akin 1976; Tracey and Cook 1977; Benzley 1974; Stern 1979).

3. Both $[\mathbf{J}]$ as well as $\frac{\partial u}{\partial \xi}$, $\frac{\partial u}{\partial \eta}$ are singular.

It should be borne in mind that the element shape functions derived for any of the above cases must satisfy the following properties:

- Inter-element (geometric) compatibility.
- Displacement continuity, and
- Ability to represent rigid-body and constant strain modes.

A particularly attractive feature of standard eight-node isoparametric (non-singular) elements is that they satisfy the above convergence criteria, and in addition also pass the patch test (Zienkiewicz 1971). Thus, the quarter-point element is widely used in linear elastic fracture computations with the finite element method.

1.1.2 Bimaterial media

For cracks in bimaterial media, the problem of a crack normal (and impinging) to a bimaterial interface and that of an interface crack are of particular importance. For a bimaterial with a crack perpendicular to the interface, the near-tip stress field is of the form $\sigma_{ij} \sim r^{-\lambda}$ $(0 < \lambda < 1)$ (Zak and Williams 1963; Cook and Erdogan 1972), where the exponent λ is given by the solution of a transcendental equation (Zak and Williams 1963) and is dependent on the Dundurs parameters α and β (see the Appendix). To model this behavior within finite elements, special singular finite elements have been proposed (Akin 1976; Tracey and Cook 1977; Stern 1979; Hughes and Stern 1980); however, these approaches require significant changes in existing finite element codes. Abdi and Valentin (1989) generalized the idea of quarter-point elements for modeling a $r^{-\lambda}$ stress-singularity, and improvements on this technique with respect to the optimal positioning of nodes have been recently proposed (Lim and Lee 1995; Yavari et al. 1999).

As opposed to the bimaterial crack that is normal to the interface, the interface crack between two elastic layers is of greater technological relevance—stemming from its significance in failure (debonding) along interfaces in bimaterial systems. The stress singularity in the vicinity of the crack-tip of a bimaterial interface crack is oscillatory in nature, along with the presence of an inverse $\sqrt{r}$-singularity, i.e, $\sigma_{22} + i\sigma_{11} \sim r^{-1/2} e^{i\epsilon \log r}$ (Rice 1988) (see the Appendix too). The oscillatory component introduces significant complexity in an element formulation, and hence the incorporation of the full radial dependence of the crack-tip displacement field has not been pursued within a classical finite element framework. Typically, for bimaterial interface crack problems, non-singular or quarter-point isoparametric elements are adopted in fracture computations (Shih and Asaro 1988; Matos et al. 1989; Nahta and Moran 1993).

1.2 Bimaterial interface cracks in the X-FEM

In the extended finite element method (X-FEM) (Moës et al. 1999; Daux et al. 2000), special functions are added to the finite element approximation using the notion of partition of unity (Melenk and Babuška 1996). For crack modeling in isotropic linear elasticity, a discontinuous function and the two-dimensional asymptotic crack-tip displacement fields are used to account for the crack. This enables the domain to be modeled by finite elements without explicitly meshing the crack surfaces, and hence quasi-static or fatigue crack propagation simulations can be carried out without remeshing.

The partition of unity framework satisfies two important properties which renders it as a powerful tool for local enrichment within a finite element setting:

1. means to include basis functions to better approximate the solution; and

2. automatic enforcement of continuity (conforming trial and test approximations)

The above properties provide a means to include and represent any function through the finite element approximation. Hence the relative ease by which different types of singularities (cracks in isotropic and bimaterial media) can be modeled. For instance, the modeling of a crack normal to a bimaterial interface using the X-FEM was introduced in Huang et al. (2002).

Consider a single crack in 2-dimensions. Let Γ_c be the crack surface (interior) and Λ_c the crack tip—the closure $\bar{\Gamma}_c = \Gamma_c \cup \Lambda_c$. The enriched displacement (trial and test) approximation for 2-d crack modeling is of the form (Moës et al. 1999):

$$\mathbf{u}^h(\mathbf{x}) = \sum_{I \in \mathcal{N}} N_I(\mathbf{x}) \left[\mathbf{u}_I + \underbrace{H(\mathbf{x})\mathbf{a}_I}_{I \in \mathcal{N}_\Gamma} + \underbrace{\sum_{\alpha=1}^{4} \Phi_\alpha(\mathbf{x})\mathbf{b}_I^\alpha}_{I \in \mathcal{N}_\Lambda} \right], \tag{6}$$

where $\mathbf{u}_I$ is the nodal displacement vector associated with the continuous part of the finite element solution, $\mathbf{a}_I$ is the nodal enriched degree of freedom vector associated with the Heaviside (discontinuous) function, and $\mathbf{b}_I^\alpha$ is the nodal enriched degree of freedom vector associated with the asymptotic crack-tip functions. In the above equation, $\mathcal{N}$ is the set of all nodes in the mesh; $\mathcal{N}_\Gamma$ is the set of nodes whose shape function support is cut by the crack interior Γ_c; and $\mathcal{N}_\Lambda$ is the set of nodes whose shape function support is cut by the crack tip Λ_c ($\mathcal{N}_\Gamma \cap \mathcal{N}_\Lambda = \emptyset$):

$$\mathcal{N}_\Lambda = \{n_K : n_K \in \mathcal{N}, \bar{\omega}_K \cap \Lambda_c \neq \emptyset\}, \tag{7}$$

$$\mathcal{N}_\Gamma = \{n_J : n_J \in \mathcal{N}, \omega_J \cap \Gamma_c \neq \emptyset, n_J \notin \mathcal{N}_\Lambda\}. \tag{8}$$

For further details on the parameters and nodal sets that appear in the above equation, see Sukumar and Prévost (2002).

1.2.1 Bimaterial interface crack

The bimaterial interface crack problem is illustrated in Figure 3. The Cartesian components of the near-tip asymptotic displacement fields are indicated in the Appendix. In order to model the interface crack within the X-FEM setting, we propose to use the generalized Heaviside functions $H(\mathbf{x})$ to model the crack interior (Γ_c), and the asymptotic crack-tip functions [$\Phi_\alpha(\mathbf{x})$, $\alpha = 1$–12] to model the crack-tip (Λ_c) for an interface crack. These functions must span the near-tip displacement field given in

Eq. (11). From Eq. (11), we can write the near-tip crack enrichment functions as:

$$
\begin{aligned}
[\Phi_\alpha(\mathbf{x}),\ \alpha = 1\text{–}12] = \{ & \sqrt{r}\cos(\epsilon\log r)e^{-2\epsilon\theta}\sin\frac{\theta}{2},\ \sqrt{r}\cos(\epsilon\log r)e^{-2\epsilon\theta}\cos\frac{\theta}{2}, \\
& \sqrt{r}\cos(\epsilon\log r)\sin\frac{\theta}{2},\ \sqrt{r}\cos(\epsilon\log r)\cos\frac{\theta}{2}, \\
& \sqrt{r}\cos(\epsilon\log r)\sin\frac{\theta}{2}\sin\theta,\ \sqrt{r}\cos(\epsilon\log r)\cos\frac{\theta}{2}\sin\theta, \\
& \sqrt{r}\sin(\epsilon\log r)e^{-2\epsilon\theta}\sin\frac{\theta}{2},\ \sqrt{r}\sin(\epsilon\log r)e^{-2\epsilon\theta}\cos\frac{\theta}{2}, \\
& \sqrt{r}\sin(\epsilon\log r)\sin\frac{\theta}{2},\ \sqrt{r}\sin(\epsilon\log r)\cos\frac{\theta}{2}, \\
& \sqrt{r}\sin(\epsilon\log r)\sin\frac{\theta}{2}\sin\theta,\ \sqrt{r}\sin(\epsilon\log r)\cos\frac{\theta}{2}\sin\theta\},
\end{aligned} \tag{9}
$$

where r and θ are polar coordinates in the local crack-tip coordinate system. The above functions span the displacement field given in the Appendix.

If the bimaterial constant $\epsilon = 0$ (isotropic material), the enrichment function reduces to

$$
[\Phi_\alpha(\mathbf{x}),\ \alpha = 1\text{–}4] = \left[\sqrt{r}\sin\frac{\theta}{2},\ \sqrt{r}\cos\frac{\theta}{2},\ \sqrt{r}\sin\frac{\theta}{2}\sin\theta,\ \sqrt{r}\cos\frac{\theta}{2}\sin\theta\right] \tag{10}
$$

which is the near-tip enrichment function used in the X-FEM to model a crack in isotropic media (Moës et al. 1999).

The complexity and nonlinear nature of the enrichment functions in Eq. (9) require additional care in the X-FEM implementation. Notably, the following issues might need to be addressed:

- Linear independence of the enrichment functions (locally within an element) so that a well-conditioned and non-singular stiffness matrix is obtained.
- Order of quadrature required to carry out the accurate numerical integration of the bilinear form.
- Solving some benchmark interface crack problems to ascertain if these enrichment functions do provide a substantial improvement over classical FEM to compute K_I^* and K_{II}^*.

References

Abdi, R. E. and G. Valentin (1989). Isoparametric elements for crack normal to the bi-material interface. *Computers and Structures 33*, 241–248.

Akin, J. E. (1976). The generation of elements with singularities. *International Journal for Numerical Methods in Engineering 10*, 1249–1259.

Barsoum, R. S. (1976). On the use of isoparametric finite elements in linear fracture mechanics. *International Journal for Numerical Methods in Engineering 10*, 551–564.

Barsoum, R. S. (1977). Triangular quarter-point elements as elastic and perfectly-plastic crack tip elements. *International Journal for Numerical Methods in Engineering 11*, 85–98.

Benzley, S. E. (1974). Representation of singularities with isoparametric finite elements. *International Journal for Numerical Methods in Engineering 8*, 537–545.

Cook, T. S. and F. Erdogan (1972). Stresses in bonded materials with a crack perpendicular to the crack. *International Journal of Engineering Sciences 10*, 677–697.

Daux, C., N. Moës, J. Dolbow, N. Sukumar, and T. Belytschko (2000). Arbitrary cracks and holes with the extended finite element method. *International Journal for Numerical Methods in Engineering 48*(12), 1741–1760.

Dundurs, J. (1969). Edge-bonded dissimilar orthogonal elastic wedges. *Journal of Applied Mechanics 36*, 650–652.

Gifford, Jr., L. N. and P. D. Hilton (1978). Stress intensity factors by enriched finite elements. *Engineering Fracture Mechanics 10*, 485–496.

Henshell, R. D. and K. G. Shaw (1975). Crack tip finite elements are unnecessary. *International Journal for Numerical Methods in Engineering 9*, 495–507.

Huang, R., J. H. Prévost, Z. Y. Huang, and Z. Suo (2002, September). Channel-cracking of thin films with the extended finite element method. *Engineering Fracture Mechanics*. submitted.

Hughes, T. J. R. and M. Stern (1980). Techniques for developing special finite element shape functions with particular references to singularities. *International Journal for Numerical Methods in Engineering 15*, 733–751.

Lim, W.-K. and C.-S. Lee (1995). Evaluation of stress intensity factors for a crack normal to a bimaterial interface using isoparamteric finite elements. *Engineering Fracture Mechanics 62*, 65–70.

Matos, P. P. L., R. M. McMeeking, P. G. Charalambides, and M. D. Drory (1989). A method for calculating stress intensities in bimaterial fracture. *International Journal of Fracture 40*, 235–254.

Melenk, J. M. and I. Babuška (1996). The partition of unity finite element method: Basic theory and applications. *Computer Methods in Applied Mechanics and Engineering 139*, 289–314.

Moës, N., J. Dolbow, and T. Belytschko (1999). A finite element method for crack growth without remeshing. *International Journal for Numerical Methods in Engineering 46*(1), 131–150.

Nahta, R. and B. Moran (1993). Domain integrals for axisymmetric interface crack problems. *International Journal of Solids and Structures 30*(15), 2027–2040.

Rice, J. R. (1988). Elastic fracture mechanics concepts for interfacial cracks. *Journal of Applied Mechanics 55*, 98–103.

Shih, C. F. and R. J. Asaro (1988). Elastic-plastic analysis of cracks on bimaterial interfaces: Part I—small scale yielding. *Journal of Applied Mechanics 55*, 299–316.

Stern, M. (1979). Families of consistent elements with singular derivative fields. *International Journal for Numerical Methods in Engineering 14*, 409–422.

Sukumar, N. and J.-H. Prévost (2002). Modeling discontinuities and their evolution with the extended finite element method. Part I: Computer implementation. *International Journal of Solids and Structures*. to be submitted.

Tracey, D. M. and T. S. Cook (1977). Analysis of power type singularities using finite elements. *International Journal for Numerical Methods in Engineering 11*, 1225–1233.

Yavari, A., S. Sarkani, and E. T. Moyer, Jr. (1999). On quadratic isoparametric transition elements for a crack normal to a bimaterial interface. *International Journal for Numerical Methods in Engineering 46*, 457–469.

Zak, A. R. and M. L. Williams (1963). Crack point singularities at a bimaterial interface. *Journal of Applied Mechanics 30*, 142–143.

Zienkiewicz, O. C. (1971). *The Finite Element Method in Engineering Science.* London: McGraw-Hill.

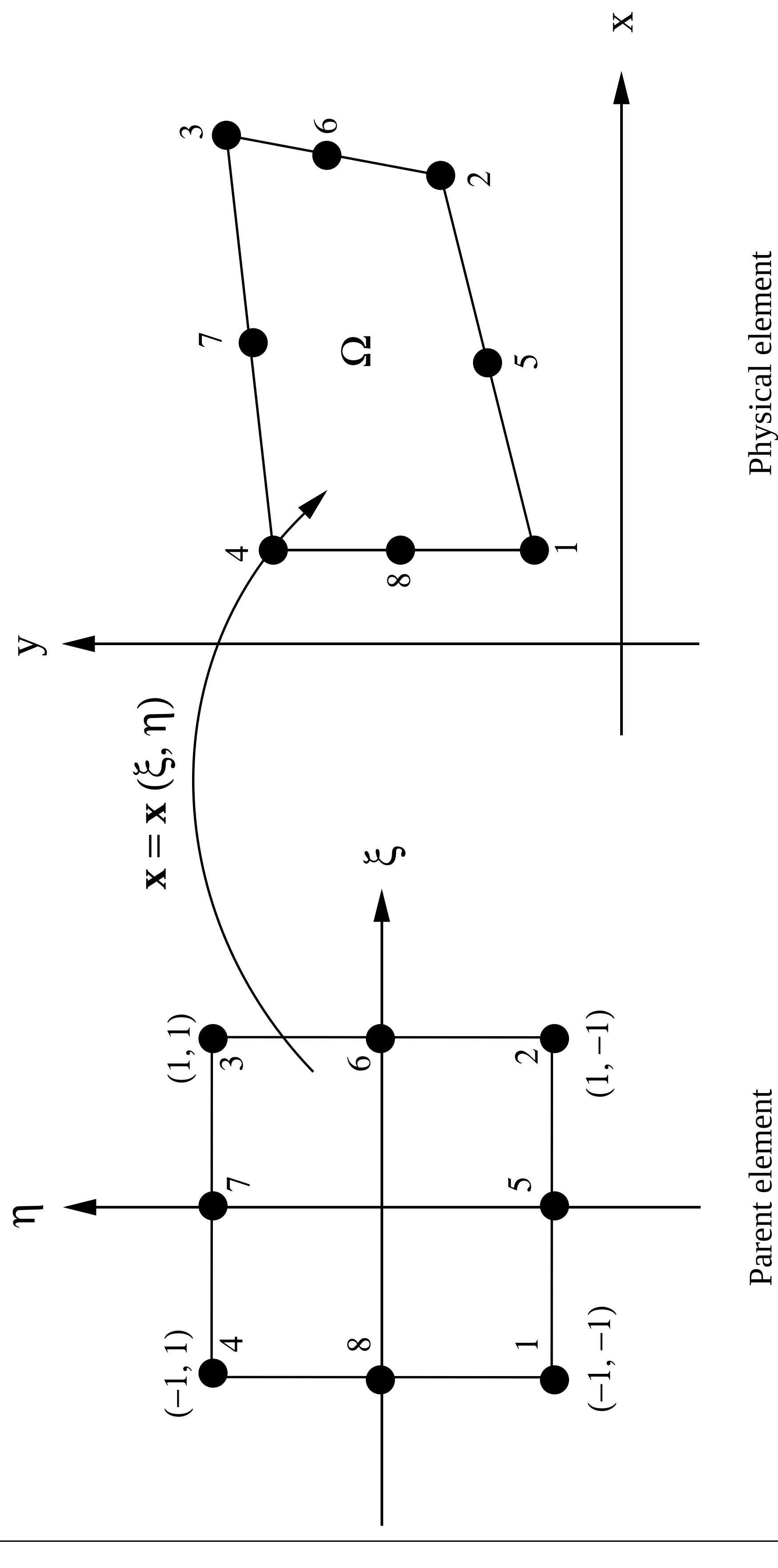

Figure 1: Mapping from ξ-space to **x**-space

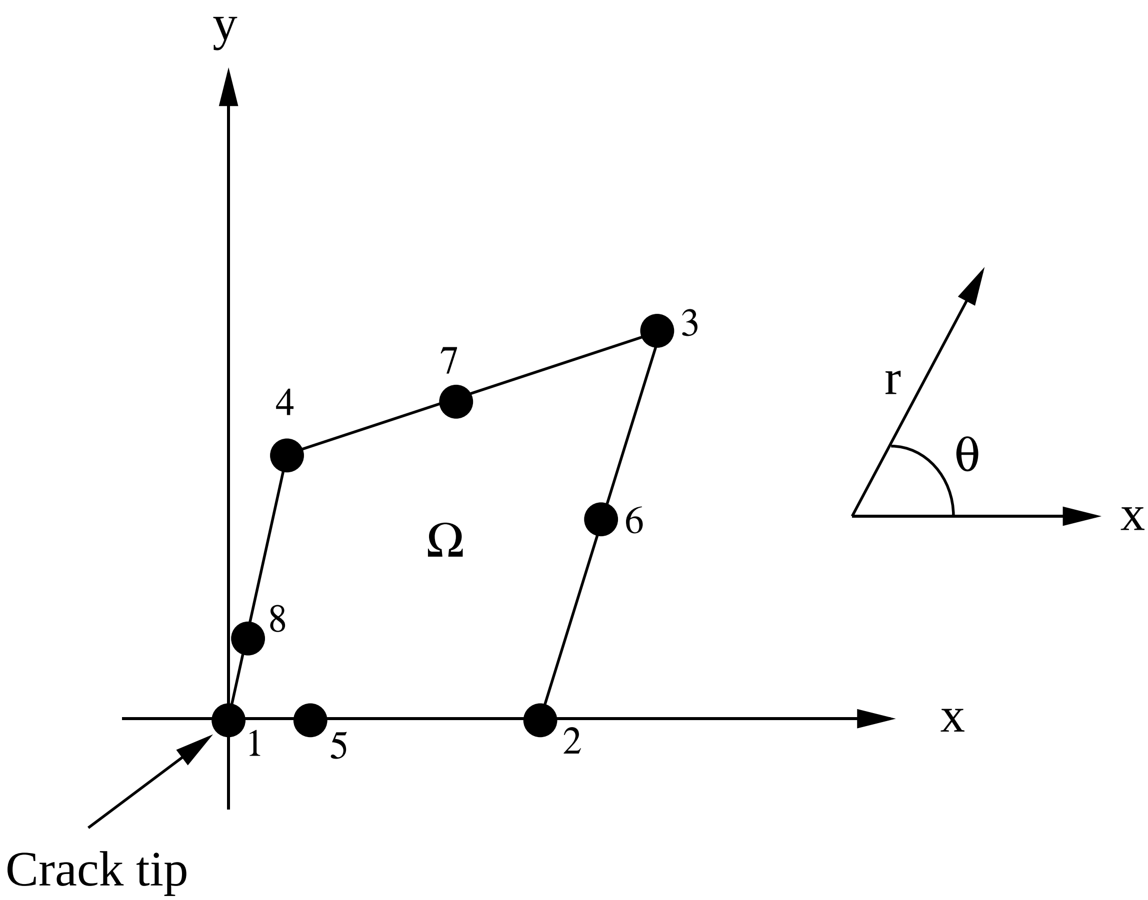

Figure 2: Quadrilateral quarter-point element.

APPENDIX

The crack-tip displacement fields in the upper-half plane (replace $\epsilon\pi$ by $-\epsilon\pi$ for the lower-half plane) for a bimaterial interface crack (Figure 3) are given in Rice (1988):

$$u_i = \frac{1}{2\mu_i}\sqrt{\frac{r}{2\pi}}\left\{\mathtt{Re}[\mathbf{K}r^{i\epsilon}]\tilde{u}_i^I(\theta,\epsilon,\nu_1) + \mathtt{Im}[\mathbf{K}r^{i\epsilon}]\tilde{u}_i^{II}(\theta,\epsilon,\nu_1)\right\} \ \ (i = x, y), \tag{11}$$

where the universal angular functions are indicated below (derived by *Dr. Zhenyu Huang*):

$$\tilde{u}_x{}^{I} = -e^{2\pi\epsilon-2\epsilon\theta}\left(\mathrm{Cos}\left[\frac{\theta}{2}\right] + 2\,\epsilon\,\mathrm{Sin}\left[\frac{\theta}{2}\right]\right) + \kappa\left(\mathrm{Cos}\left[\frac{\theta}{2}\right] - 2\,\epsilon\,\mathrm{Sin}\left[\frac{\theta}{2}\right]\right) + (1+4\,\epsilon^2)\,\mathrm{Sin}\left[\frac{\theta}{2}\right]\,\mathrm{Sin}[\theta];$$

$$\tilde{u}_y{}^{I} = e^{2\,\epsilon\,(\pi-\theta)}\left(\mathrm{Sin}\left[\frac{\theta}{2}\right] - 2\,\epsilon\,\mathrm{Cos}\left[\frac{\theta}{2}\right]\right) + \kappa\left(\mathrm{Sin}\left[\frac{\theta}{2}\right] + 2\,\epsilon\,\mathrm{Cos}\left[\frac{\theta}{2}\right]\right) - (1+4\,\epsilon^2)\,\mathrm{Cos}\left[\frac{\theta}{2}\right]\,\mathrm{Sin}[\theta];$$

$$\tilde{u}_x{}^{II} = e^{2\pi\epsilon-2\epsilon\theta}\left(\mathrm{Sin}\left[\frac{\theta}{2}\right] - 2\,\epsilon\,\mathrm{Cos}\left[\frac{\theta}{2}\right]\right) + \kappa\left(\mathrm{Sin}\left[\frac{\theta}{2}\right] + 2\,\epsilon\,\mathrm{Cos}\left[\frac{\theta}{2}\right]\right) + (1+4\,\epsilon^2)\,\mathrm{Cos}\left[\frac{\theta}{2}\right]\,\mathrm{Sin}[\theta];$$

$$\tilde{u}_y{}^{II} = e^{2\,\epsilon\,(\pi-\theta)}\left(\mathrm{Cos}\left[\frac{\theta}{2}\right] + 2\,\epsilon\,\mathrm{Sin}\left[\frac{\theta}{2}\right]\right) - \kappa\left(\mathrm{Cos}\left[\frac{\theta}{2}\right] - 2\,\epsilon\,\mathrm{Sin}\left[\frac{\theta}{2}\right]\right) + (1+4\,\epsilon^2)\,\mathrm{Sin}\left[\frac{\theta}{2}\right]\,\mathrm{Sin}[\theta];$$

In the equations for the displacement field, α and β are the Dundurs parameters (Dundurs 1969) and ϵ is the bimaterial constant:

$$\alpha = \frac{\mu_1(\kappa_2+1) - \mu_2(\kappa_1+1)}{\mu_1(\kappa_2+1) + \mu_2(\kappa_1+1)}, \quad \beta = \frac{\mu_1(\kappa_2-1) - \mu_2(\kappa_1-1)}{\mu_1(\kappa_2+1) + \mu_2(\kappa_1+1)}, \tag{12a}$$

$$\epsilon = \frac{1}{2\pi} \log\left(\frac{1-\beta}{1+\beta}\right), \tag{12b}$$

$$\kappa_i = \begin{cases} \dfrac{3-\nu_i}{1+\nu_i} & \text{(plane stress)} \\ 3-4\nu_i & \text{(plane strain)} \end{cases}, \tag{12c}$$

where μ_i and ν_i are the shear modulus and the Poisson's ratio, respectively, of material i $(i = 1, 2)$.

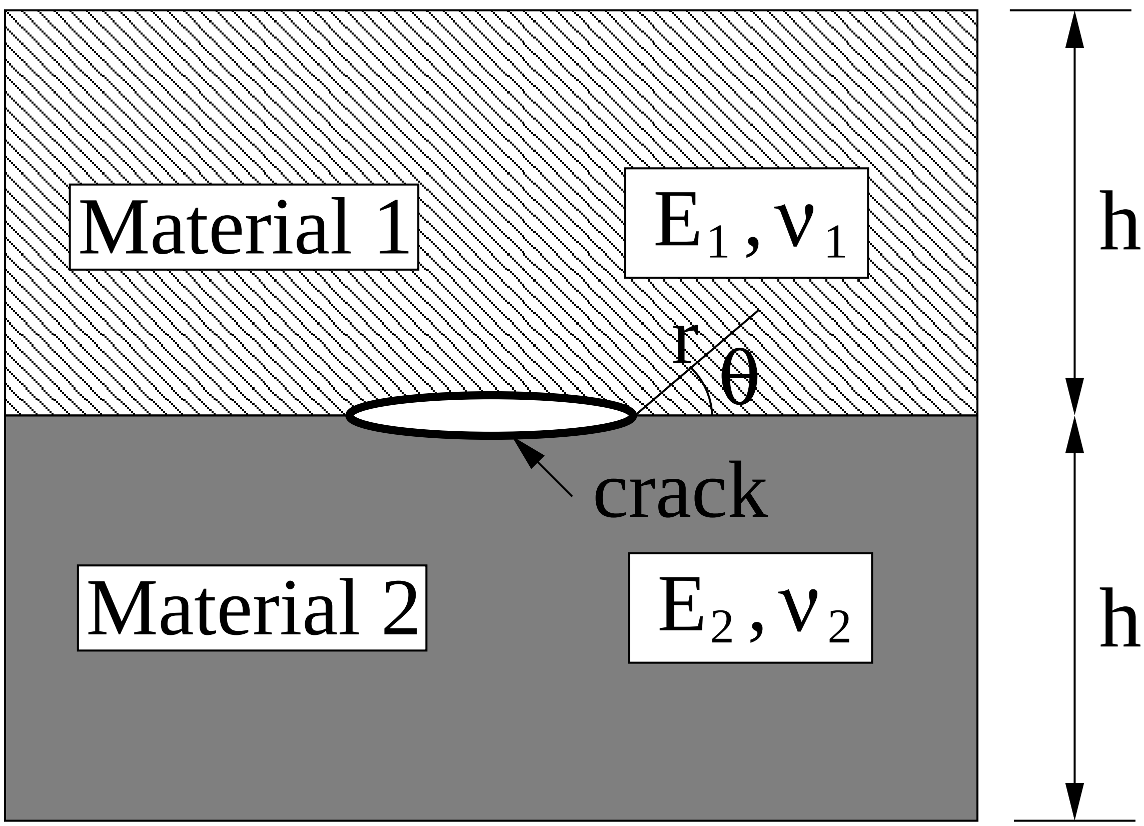

Figure 3: Bimaterial interface crack.